Cripto regulates skeletal muscle regeneration and modulates satellite cell determination by antagonizing myostatin

Ombretta Guardiola[a,b,1], Peggy Lafuste[c,d,e,1], Silvia Brunelli[f,g,2], Salvatore Iaconis[a,b,2], Thierry Touvier[h], Philippos Mourikis[i], Katrien De Bock[c,d], Enza Lonardo[a,b], Gennaro Andolfi[a,b], Ann Bouché[c], Giovanna L. Liguori[b], Michael M. Shen[j], Shahragim Tajbakhsh[i], Giulio Cossu[k], Peter Carmeliet[c,d,3], and Gabriella Minchiotti[a,b,3,4]

[a]Stem Cell Fate Laboratory, Institute of Genetics and Biophysics "Adriano Buzzati-Traverso," Consiglio Nazionale delle Ricerche, 80131 Naples, Italy; [b]Institute of Genetics and Biophysics "Adriano Buzzati-Traverso," Consiglio Nazionale delle Ricerche, 80131 Naples, Italy; [c]Laboratory of Angiogenesis and Neurovascular Link, Vesalius Research Center, Flemish Institute of Biotechnology, 3000 Leuven, Belgium; [d]Laboratory of Angiogenesis and Neurovascular Link, Vesalius Research Center, Department of Oncology, University of Leuven, 3000 Leuven, Belgium; [e]Institut National de la Santé et de la Recherche Médicale, U955, Team 10 "Cell Interactions in the Neuromuscular System," University Paris Est Creteil, F-94000 Creteil, France; [f]Division of Regenerative Medicine, San Raffaele Scientific Institute, 20132 Milan, Italy; [g]Department of Experimental Medicine, University of Milano-Bicocca, 20052 Monza, Italy; [h]Eugenio Medea Scientific Institute, 23842 Bosisio Parini, Italy; [i]Stem Cells and Development Unit, Institut Pasteur, Centre National de la Recherche Scientifique, Unité de Recherche Associée, 2578 Paris, France; [j]Departments of Medicine and Genetics & Development, Herbert Irving Comprehensive Cancer Center, Columbia University Medical Center, New York, NY 10032; and [k]Department of Cell and Developmental Biology, University College London, London WC1E 6DE, United Kingdom

Edited by Eric N. Olson, University of Texas Southwestern Medical Center, Dallas, TX, and approved October 4, 2012 (received for review March 9, 2012)

Skeletal muscle regeneration mainly depends on satellite cells, a population of resident muscle stem cells. However, our understanding of the molecular mechanisms underlying satellite cell activation is still largely undefined. Here, we show that Cripto, a regulator of early embryogenesis, is a novel regulator of muscle regeneration and satellite cell progression toward the myogenic lineage. Conditional inactivation of *cripto* in adult satellite cells compromises skeletal muscle regeneration, whereas gain of function of Cripto accelerates regeneration, leading to muscle hypertrophy. Moreover, we provide evidence that Cripto modulates myogenic cell determination and promotes proliferation by antagonizing the TGF-β ligand myostatin. Our data provide unique insights into the molecular and cellular basis of Cripto activity in skeletal muscle regeneration and raise previously undescribed implications for stem cell biology and regenerative medicine.

myogenic commitment | skeletal muscle stem cells | teratocarcinoma derived growth factor-1 (TDGF-1) | growth differentiation factor-8 (GDF-8)

It is now evident that genes and molecular mechanisms, which have key roles during embryogenesis, are reactivated in the adult during tissue remodeling and regeneration and that when deregulated, they may contribute to cancer progression (1). The *cripto* gene has emerged as a key player in this complex scenario. Cripto is a GPI-anchored protein and the founder member of a family of signaling molecules, the EGF-CFC proteins, important for vertebrate development (2). Cripto is associated with the pluripotent status of both human and mouse ES cells (ESCs) (3), and it acts as a key player in the signaling networks orchestrating ESC differentiation (4). Intriguingly, it has been recently suggested that Cripto may serve as a regulator to control dormancy of hematopoietic stem cells (5).

Under normal physiological conditions, Cripto is expressed during embryonic development (2), and it has been shown to have activity both as a soluble factor and as a GPI-anchored protein (6–8). Existing models indicate that Cripto can function via different signaling pathways. Cripto plays distinct and opposing roles in modulating the activity of several TGF-β ligands. Indeed, as an obligate coreceptor, Cripto binds Nodal and GDF1/GDF3 and stimulates signaling through the activin receptor complex composed of type I serine-threonine ActRIB (ALK4) and type II receptor (ActRII/ActRIIB) (9–11). Following receptor activation, the intracellular effectors Smad2 and/or Smad3 are phosphorylated and accumulate in the nucleus with Smad4 to mediate transcriptional response (12). In contrast to its coreceptor function, Cripto is able to antagonize signaling of other members of the TGF-β family (i.e., activins and TGF-β). This inhibitory activity of Cripto results in a reduced ability to form an active ActRII/ActRIB receptor complex (13–15).

Despite the well-described role of Cripto in early development and ESC differentiation, the role of this protein in postnatal life remains elusive. To date, de novo expression of Cripto has been associated with several epithelial cancers (16, 17), but its role in other pathological conditions, such as injury or degenerative diseases, has not been investigated. Given the physiological activity of Cripto in the instructive events of embryonic mesodermal commitment and differentiation (4), we hypothesized that Cripto expression might be reactivated in response to injury in mesenchymal tissues, such as skeletal muscles.

Adult skeletal muscle generally has a low cellular turnover rate. However, in response to certain pathological conditions, it undergoes robust regeneration. Regeneration is mainly dependent on satellite cells, a population of resident stem cells that are in a quiescent state during muscle homeostasis. After injury or disease, satellite cells become activated, proliferate, migrate to the site of injury, and either fuse to form multinucleated myotubes or reestablish a self-renewing pool of quiescent satellite cells (18). Quiescent satellite cells express the transcription factor Pax7, which is involved in myogenic specification (19, 20). Following injury, activated satellite cells start proliferating and expressing MyoD, whereas Pax7 expression is progressively reduced. Subsequently, expression of myogenin and MRF4 (muscle regulatory factor 4 or muscle regulatory transcription factor 4) is up-regulated as cells enter their terminal differentiation program. A fraction of activated cells down-regulate expression of MyoD and return to cellular quiescence to maintain a pool of satellite cells (21). A delicate balance between satellite cell proliferation and exit from cell cycle,

Author contributions: O.G., P.L., and G.M. designed research; O.G., P.L., S.B., S.I., T.T., E.L., G.A., and A.B. performed research; P.M., G.L.L., M.M.S., S.T., and P.C. contributed new reagents/analytic tools; O.G., P.L., S.B., S.I., K.D.B., S.T., G.C., P.C., and G.M. analyzed data; and G.M. wrote the paper.

The authors declare no conflict of interest.

This article is a PNAS Direct Submission.

[1]O.G. and P.L. contributed equally to this work.

[2]S.B. and S.I. contributed equally to this work.

[3]P.C. and G.M. contributed equally to this work.

[4]To whom correspondence should be addressed. E-mail: gabriella.minchiotti@igb.cnr.it.

See Author Summary on page 19051 (volume 109, number 47).

This article contains supporting information online at www.pnas.org/lookup/suppl/doi:10.1073/pnas.1204017109/-/DCSupplemental.

differentiation, and fusion is required for the correct muscle regeneration to occur. Although some signaling molecules have been found to play a crucial role in these processes (11), including hepatocyte growth factor (22), insulin-like growth factors (23), myostatin (24), and Wnts (25), the underlying molecular mechanisms of muscle regeneration remain largely undefined.

In the present study, we provide evidence that Cripto is reexpressed in adult skeletal muscle in response to injury and that this response correlates with and regulates muscle regeneration. We also show that Cripto is expressed in activated satellite cells and promotes myogenic cell determination and proliferation by antagonizing TGF-β ligand myostatin.

Results

Cripto Is Expressed During Skeletal Muscle Regeneration and in Myogenic Cells in Vivo and ex Vivo. To evaluate whether Cripto is activated in adult tissues under pathological conditions, we performed double immunofluorescence analysis for Cripto and laminin on normal adult skeletal muscle both during homeostasis and after cardiotoxin (CTX)-induced injury. Cripto was undetectable in healthy uninjured muscles (Fig. 1 *A–C*); in contrast, strong expression of Cripto was observed in the regenerating area both inside and outside of the basement membrane surrounding myofibers (Fig. 1 *D–F*). Cripto expression was confirmed by flow cytometry (FACS) analysis (Fig. S1*A*). Notably, expression of *cripto* progressively decreases during the regeneration process (Fig. S1 *C–F*). To assess whether different cell types that take part in the regeneration process expressed Cripto, we performed double staining with specific markers. Immunofluorescence analysis revealed that Cripto was expressed in myogenic cells, as indicated by coexpression with MyoD (Figs. 1 *G–I*). In addition, double staining with F4/80, a macrophage-specific membrane antigen, showed that Cripto was expressed in inflammatory cells (Fig. 1 *J–L*). FACS analysis on dissociated muscle cells confirmed that at day 4 after CTX injection, 15.2% of Cripto$^+$ cells are F4/80$^+$ (Fig. S1*B*).

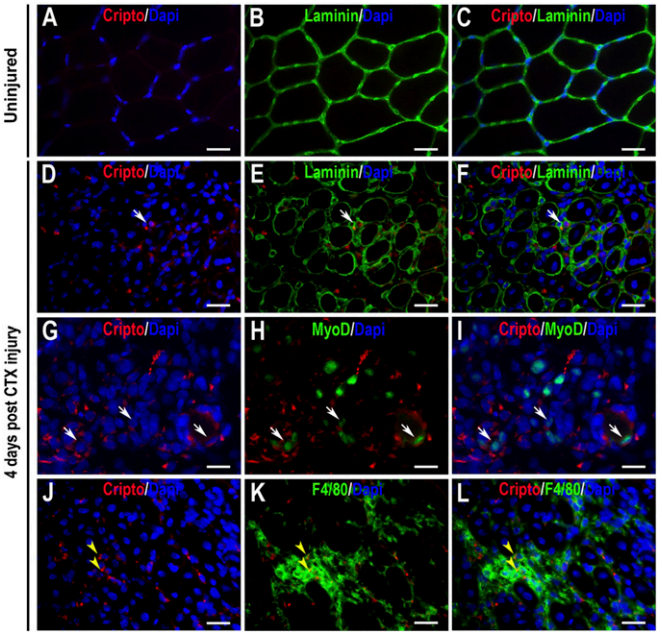

Fig. 1. Cripto is expressed during skeletal muscle regeneration. Double immunofluorescence with anti-laminin (green) and anti-Cripto (red) antibodies is illustrated in uninjured TA muscle (*A–C*) and in CTX-injured TA muscles during regeneration (*D–F*), showing Cripto expression in regenerating fibers (white arrows). (*G–L*) Regenerating muscle sections stained with anti-Cripto (red) and anti-MyoD or F4/80 (green) antibodies. Colocalization of Cripto and MyoD (green) or F4/80 (green) indicates Cripto expression in myogenic cells (*G–I*, white arrows) and inflammatory cells (*J–L*, yellow arrowheads), respectively. Nuclei are stained in blue with DAPI. (Scale bars = 50 μm.) See also Fig. S1.

Expression of *cripto* during muscle regeneration and in satellite cell progeny after activation raised the intriguing possibility that *cripto* might play a role in regulating myogenic cell behavior. To address this issue in more detail, we used single-myofiber preparations isolated from WT myofibers (26) and performed a time course immunofluorescence analysis for Cripto, Pax7, and MyoD. Immediately after plating at time 0 (T0), Cripto expression was undetectable in Pax7$^+$/MyoD$^-$ satellite cells (Fig. 2 *A–E′*). Interestingly, Cripto started to be detected, along with Pax7 and MyoD (Fig. 2 *F–J′*), as early as after 24 h (T24), persisting after 48 h (T48) in culture (Fig. 2 *K–O′*). We then extended our analysis using myofibers isolated from *Myf5*$^{nlacZ/+}$ mice (27), which express a nuclear localized *lacZ* (*nlacZ*) reporter gene targeted to the *Myf5* locus (28). Double staining for Cripto and β-galactosidase (β-gal) showed Cripto expression, along with β-gal expression (Fig. S2 *A–D*). Moreover, Cripto expression persisted in satellite cells detaching from the fibers after 60 h in culture (Fig. S2 *E–L*).

Taken together, our data provide evidence that Cripto is expressed in activated satellite cells committed to the myogenic lineage, persisting in proliferating transient amplifying myoblasts.

Conditional Targeted Deletion of *Cripto* in Adult Satellite Cells Affects Skeletal Muscle Regeneration. These results prompted us to evaluate whether Cripto might have a physiological role in skeletal muscle regeneration in vivo, using a loss-of-function approach. *Cripto* null mutants die during early embryonic development (29); we thus used a Cre-Lox strategy to obtain conditional *cripto* deletion in adult mice. Moreover, to distinguish between the relative roles of Cripto in inflammatory cell and satellite cell contributions during this process, we generated a unique mouse model for conditional inactivation of *cripto* in satellite cells, *Tg:Pax7-CreERT2::Cripto*$^{loxP/-}$ mice, by crossing *Cripto*$^{loxP/-}$ mice with a tamoxifen-inducible *Tg:Pax7-CreERT2* transgenic line (30). *Tg:Pax7-CreERT2::Cripto*$^{loxP/-}$ adult mice were treated with tamoxifen or vehicle, as a control, once a day for 5 d; at day 4, tibialis anterior (TA) muscles were injected locally with CTX, and the effect on muscle regeneration was evaluated at days 4 and 15 after CTX injection (Fig. 3*A*). To verify the tissue-specific recombinase activity of Cre, we isolated and genotyped the contralateral uninjured TA muscle and the bone marrow of both tamoxifen- and vehicle-treated mice (Fig. 3*B*). As expected, the *cripto*-deleted specific band was detected in the contralateral uninjured TA muscle of the tamoxifen-treated mice but not the control mice. Notably, the *cripto*-deleted band was absent in the bone marrow genomic DNA (Fig. 3*B*), thus confirming that *cripto* deletion occurred selectively in skeletal muscle cells. Accordingly, Cripto protein levels decreased in muscle tissue of tamoxifen-treated mice compared with control mice at day 4 after injury, as shown by ELISA assays (Fig. 3*C*). Using these mice, we stained sections of the CTX-injected TA muscles with H&E to perform morphometric analysis (Fig. 3*D*). Remarkably, the myofiber cross-sectional area (CSA) was significantly reduced in the tamoxifen-treated mice compared with control mice (Fig. 3 *E* and *F*). Given that Cripto is also expressed in macrophages, our data provide direct evidence for a role of Cripto specifically in adult myogenic cells during skeletal muscle regeneration.

Cripto Overexpression Accelerates Skeletal Muscle Regeneration and Induces Myofiber Hypertrophy in Vivo. We next investigated whether Cripto might modulate acute skeletal muscle regeneration in vivo, using a gain-of-function approach. To do so, we generated a replication-deficient adenovirus, adeno (Ad)-soluble Cripto (sCripto), that can be used to overexpress a biologically active sCripto protein (31) in skeletal muscle. We first evaluated whether sCripto was sufficiently expressed on Ad-sCripto gene transfer by measuring

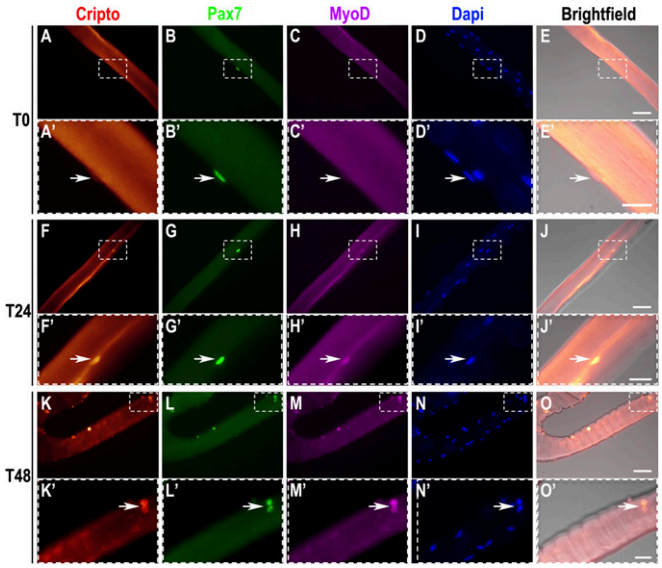

Fig. 2. Cripto is expressed in activated/proliferating satellite cells. Cripto staining with Pax7 and MyoD on teased myofibers isolated from C57BL/6 mice at different time points in culture: 0 h (*A–E*, T0), 24 h (*F–J*, T24), and 48 h (*K–O*, T48). The Cripto staining images are superimposed on a phase-contrast image (*E*, *J*, and *O*). (*Insets*, *A′–O′*) Higher magnifications of myofibers. (Scale bars = 25 μm and 50 μm.) See also Fig. S2.

Cripto protein levels in both muscles and serum. To this end, TA muscles were injected with CTX, along with either Ad-sCripto or Ad-Control (encoding an empty vector); mice were killed at different time points, and sCripto serum levels were determined using a sandwich ELISA-based assay. As early as 6 h after virus injection, sCripto was detectable in the serum of Ad-sCripto–infected mice (~5 ng/mL), which progressively decreased to reach a level of ~1 ng/mL after 6 d (Fig. S3*A*); by contrast, sCripto was undetectable in the serum of mice infected with Ad-Control. Finally, dose-dependent Cripto overexpression was also detected in Ad-sCripto–transduced muscles after 5 d, confirming that sCripto was efficiently expressed on Ad-sCripto gene transfer (Fig. S3*B*).

To analyze the overall effect of sCripto overexpression on muscle regeneration, we triggered skeletal muscle regeneration by injecting high doses of CTX (32) in WT TA muscles infected with Ad-Control or Ad-sCripto. Mice were killed 4, 8, and 22 d after CTX and adenovirus injection. We first verified Cripto overexpression in the serum and skeletal muscles by ELISA and immunofluorescence analysis, respectively (Fig. S3 *C* and *D*). Muscle sections were then stained with H&E for the morphological and morphometric analysis (Fig. 4*A*); muscle regeneration was assessed and expressed as a percentage of the area of centrally nucleated fibers compared with the total muscle section area (Fig. 4*B*) at each time point. At day 4 after injections, we did not find any significant difference between Ad-Control and Ad-sCripto–infected muscles [18.7 ± 3% after Ad-sCripto vs. 19.9 ± 4.5% after Ad-Control; $n = 5$; P = not significant (NS)]; by contrast, 8 d after the CTX injury, Ad-sCripto–infected muscles clearly exhibited more robust regeneration than control muscles (64 ± 11% after Ad-sCripto vs. 15 ± 1.2% after Ad-Control; $n = 5$ mice; $^{**}P = 0.004$; Fig. 4 *A* and *B*). By day 22 after injury, although the regeneration process was nearly completed in both conditions, muscle regeneration was still significantly improved in Ad-sCripto–treated mice (92 ± 4.6% after Ad-sCripto vs. 76 ± 4.5% after Ad-Control; $n = 5$ mice; $^{*}P = 0.04$; Fig. 4 *A* and *B*). Comparable results were obtained in models of less severe muscle damage [i.e., femoral artery ligation (Mild Limb Ischemia [MLI]) and lower doses of CTX] (Fig. S4 *A–C*). In accordance with these findings, muscles overexpressing Cripto also showed reduced necrotic areas compared with control muscles (36 ± 11% after Ad-sCripto vs. 85 ± 1.2% after Ad-Control; $n = 5$ mice; $^{**}P = 0.004$; Fig. 4*C*). Moreover, the accelerated regeneration was accompanied by high expression in

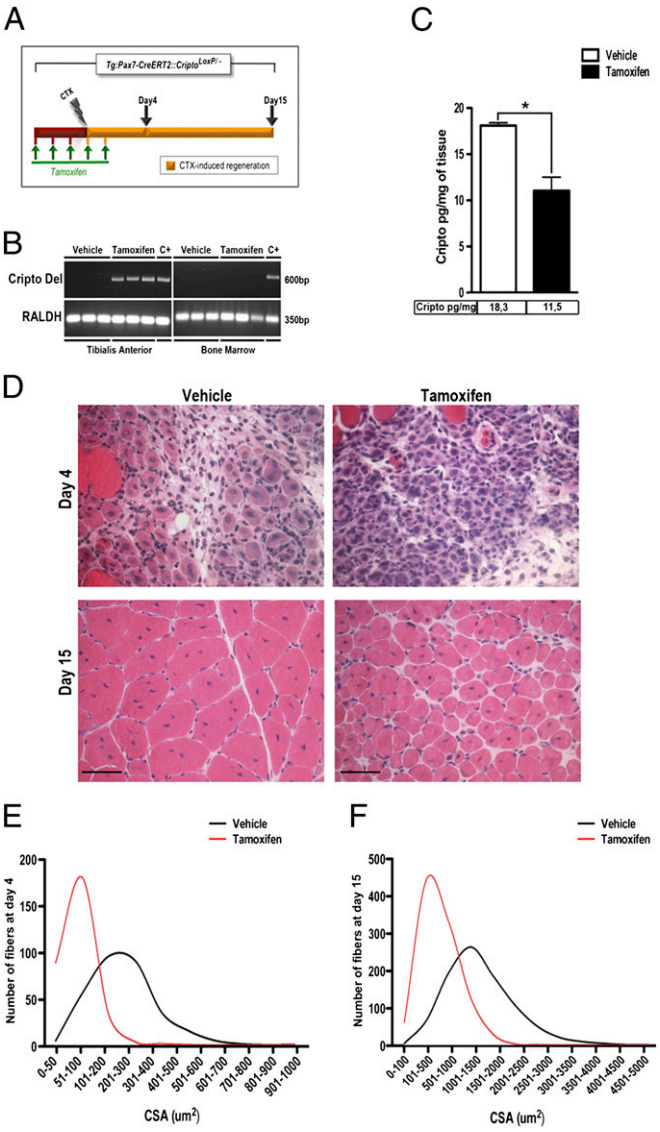

Fig. 3. Conditional targeted deletion of *cripto* in satellite cells impairs muscle regeneration after acute muscle damage. (*A*) Schematic representation of conditional loss of function of *Cripto* using *Tg:Pax7-CreERT2::Cripto*$^{loxP/-}$ mice. Tamoxifen or control vehicle was injected i.p. in adult mice (1 mo of age) once a day for 5 d. At day 4, regeneration was triggered by CTX injection in TA muscle of both groups, and analysis was performed at the indicated time points (day 4 and day 15). (*B*) PCR analysis shows tamoxifen-induced deletion of *Cripto* floxed allele (Cripto Del) only in uninjured contralateral TA muscle (*Left*) but not in bone marrow (*Right*), isolated at day 15. Genomic DNA isolated from uninjured TA muscles and bone marrow of tamoxifen-treated *Cripto*$^{loxP/loxP}$ CAG-*CreERT2* mice was used as a positive control (C+). RALDH, retinaldehyde dehydrogenase. (*C*) ELISA-based assay of Cripto protein levels in muscle tissue of *Tg:Pax7-CreERT2::Cripto*$^{loxP/-}$ mice treated with either sesame oil as a control or tamoxifen at day 4 after injury (18.1 ± 0.3 pg/mg for control vs. 11.05 ± 1.4 pg/mg for tamoxifen). Values are mean ± SEM; $n = 3$ mice per group; $^{*}P = 0.04$. (*D*) Representative H&E-stained sections of CTX-treated muscles at indicated time points. (Scale bars = 50 μm.) CSA analysis of regenerated fibers at day 4 (*E*) and at day 15 (*F*) shows smaller myofibers in tamoxifen treated mice vs. control mice at both time points. See also Table S1.

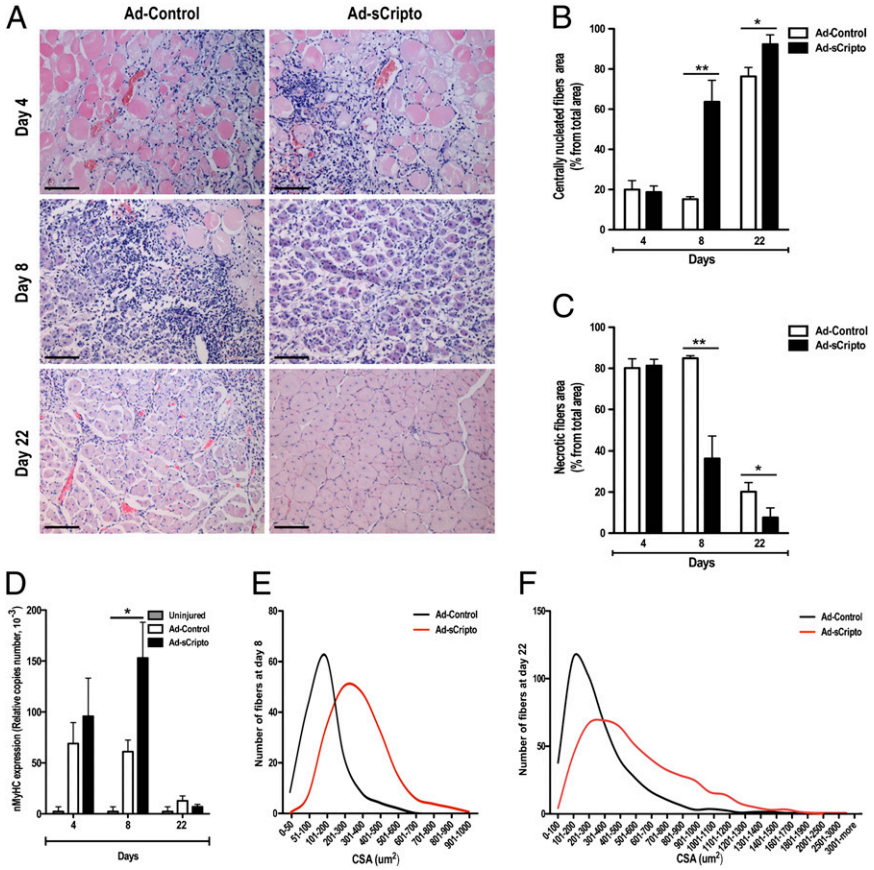

Fig. 4. Cripto overexpression accelerates muscle regeneration after acute muscle damage. (*A*) Representative photos from H&E staining of CTX-treated muscles at indicated days after injury, injected with either Ad-Control or Ad-sCripto. (Scale bars = 100 μm.) (*B* and *C*) Cripto overexpression induces faster regeneration as shown by fiber type repartition. Centrally nucleated myofibers increased in Ad-sCripto vs. Ad-Control (*B*), and the necrotic fiber area was reduced (*C*). Results are expressed as a percentage of the total section area at each time point. Values are mean ± SEM; $n = 5$ mice per group; $^{**}P < 0.005$. (*D*) qRT-PCR analysis of *nmyhc* expression. Values are mean ± SEM; $n = 5$ mice per time point; $^{**}P < 0.005$. CSA analysis of centrally nucleated fibers at day 8 (*E*) and day 22 (*F*) shows an increased percentage of large fibers in Ad-sCripto vs. control mice, indicating hypertrophy of muscle fibers. See also Figs. S3 and S4 and Table S2.

Ad-sCripto muscles of neonatal myosin heavy chain (*nmyhc*), a marker of muscle regeneration in the adult. Expression of *nmyhc*, analyzed by quantitative real-time PCR (qRT-PCR), was significantly increased in Ad-sCripto mice at day 8 (Fig. 4*D*). Most remarkably, morphometric analysis (CSA) showed that Cripto overexpression increased myofiber size at both 8 and 22 d after the CTX injury (Fig. 4 *E* and *F*, respectively), and results were confirmed in the model of less severe muscle damage (Fig. S4*C*).

Taken together, our data indicate that sCripto overexpression accelerates muscle regeneration and induces myofiber hypertrophy following acute skeletal muscle damage. Among the different processes active in muscle healing and regeneration, inflammation plays an important role. Because Cripto was also expressed in macrophages during regeneration (Fig. 1 *J–L*), we compared the degree of inflammation in TA muscles transduced with Ad-sCripto and Ad-Control. Immunostaining for F4/80 followed by morphometric analysis showed that there was no significant difference in the $F4/80^+$ inflammatory cell area in the two groups (3.7 ± 2% after Ad-sCripto vs. 4.6 ± 1% after Ad-Control on day 4; 9.1 ± 4% after Ad-sCripto vs. 5.2 ± 3% after Ad-Control on day 8; 5.7 ± 2% after Ad-sCripto vs. 6.9 ± 3% after Ad-Control on day 22; $n = 5$ mice per group; P = NS; Fig. S4*C*), thus suggesting that Cripto overexpression does not substantially contribute to modulation of the inflammatory process.

sCripto Rescues Muscle Regeneration in Mice with Conditional Targeted Deletion of *cripto* in Adult Satellite Cells. To evaluate whether sCripto was able to recapitulate the function of endogenous membrane Cripto (mCripto) fully in vivo, we investigated whether sCripto rescued muscle regeneration defects in mice with genetic ablation of *cripto* in adult satellite cells. To this end, *Tg:Pax7-CreERT2::Cripto*$^{loxP/-}$ and control *Cripto*$^{loxP/-}$ mice were injected i.p. with tamoxifen once a day for 5 d. At day 4, regeneration was triggered in TA muscles by CTX injection, along with local infection of either Ad-sCripto or Ad-Control, and the effect on muscle regeneration was evaluated at day 4 after injury (Fig. 5*A*). We first verified by PCR analysis that *cripto* deletion occurred selectively in skeletal muscles of *Tg:Pax7-CreERT2::Cripto*$^{loxP/-}$ mice (Fig. S4*E*). Accordingly, endogenous Cripto protein levels decreased in muscle tissue of *Tg:Pax7-CreERT2::Cripto*$^{loxP/-}$ mice compared with control *Cripto*$^{loxP/-}$ mice, as shown by ELISA (Fig. 5*B*). As expected, we found that Cripto protein levels strongly increased in Ad-sCripto–transduced muscles compared with Ad-Control (Fig. 5*B*). We thus performed morphometric analysis of myofiber size in the different mouse groups. As expected, the myofiber CSA was significantly reduced in *Tg:Pax7-CreERT2::Cripto*$^{loxP/-}$ mice compared with *Cripto*$^{loxP/-}$ control mice. Most remarkably, this reduction was fully rescued by sCripto overexpression in *Tg:Pax7-CreERT2::Cripto*$^{loxP/-}$ mice, and the CSA eventually increased compared with that in *Cripto*$^{loxP/-}$ control mice, thus providing direct evidence that sCripto was able to

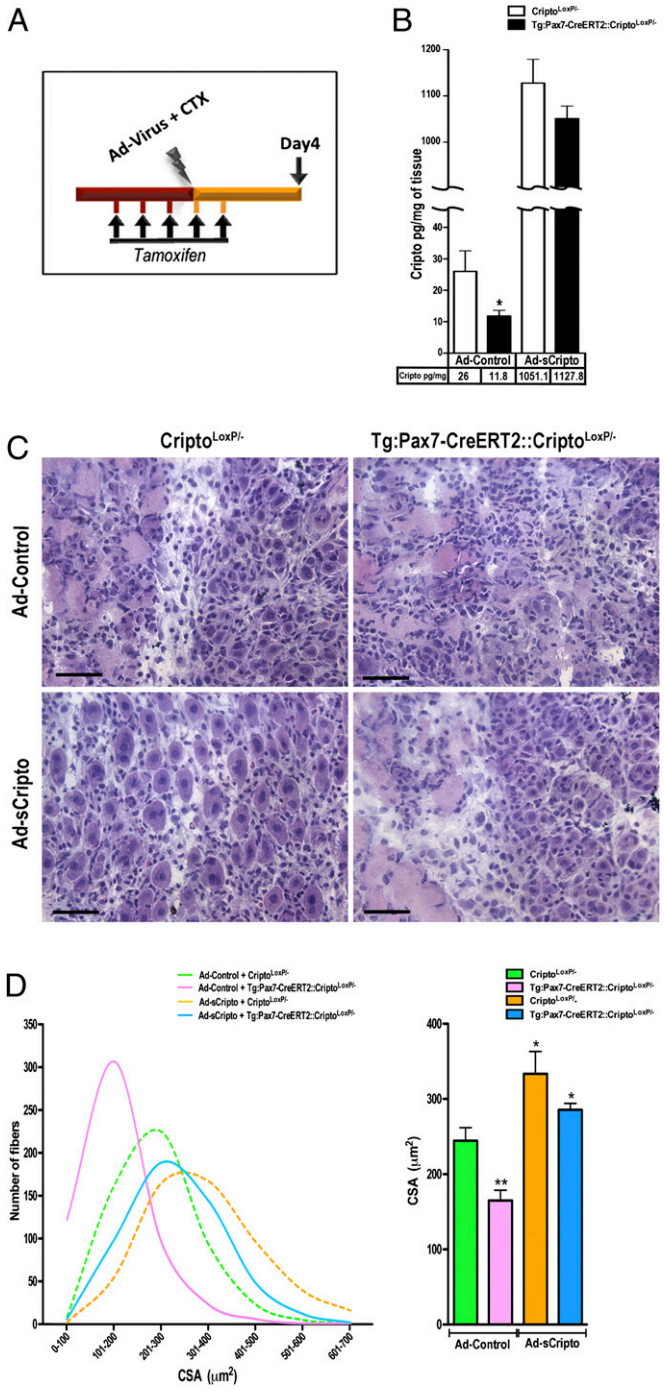

Fig. 5. sCripto rescues muscle regeneration in a mouse model of conditional targeted deletion of *cripto* in adult satellite cells. (*A*) Schematic representation of conditional loss of function of *cripto* in adult satellite cells, along with adenoviral-mediated sCripto overexpression, in *Tg:Pax7-CreERT2::Cripto*$^{loxP/-}$ and *Cripto*$^{loxP/-}$ mice. (*B*) ELISA of Cripto protein levels in muscle tissue at day 4 after injury. Average Cripto levels are plotted for each group/condition. Endogenous Cripto protein was significantly reduced on targeted deletion of *cripto* in *Tg:Pax7-CreERT2::Cripto*$^{loxP/-}$ compared with *Cripto*$^{loxP/-}$ control, both infected with Ad-Control (26 ± 6.5 pg/mg *Cripto*$^{loxP/-}$ vs. 11.8 ± 1.8 pg/mg *Tg:Pax7-CreERT2::Cripto*$^{loxP/-}$; $*P = 0.05$). Cripto levels increased (~1 ng/mg) in Ad-sCripto–infected mice. Values are mean ± SEM; $n = 3$ mice per group. (*C*) Representative H&E staining of TA muscle sections from each group. (Scale bars = 50 μm.) (*D*) Myofiber CSA distribution and average were reduced in Ad-Control–treated *Tg:Pax7-CreERT2::Cripto*$^{loxP/-}$ mice (pink line and bar) compared with *Cripto*$^{loxP/-}$ (green line and bar) and were increased on sCripto overexpression (blue line and bar). Myofiber CSA distribution and average increased in control *Cripto*$^{loxP/-}$ mice overexpressing sCripto (orange line and bar) compared with Ad-Control (green line and bar). Values are mean ± SEM; $n = 3$ mice/group; $*P = 0.02$; $**P < 0.004$. See also Fig. S4.

recapitulate fully the function of the endogenous mCripto in satellite cells. Furthermore, sCripto overexpression increased myofiber CSA also in control *Cripto*$^{loxP/-}$ mice (Fig. 5 *C* and *D*), thus confirming the positive effect of sCripto in muscle regeneration and supporting our conclusion.

Cripto Promotes Myogenic Cell Proliferation. Results of gain-of-function and loss-of-function experiments suggest that Cripto might play a role in regulating satellite cell function and, eventually, modulate skeletal muscle regeneration. To gain more insight into this issue, we first evaluated whether Cripto would be mitogenic for primary myoblasts in culture. To this end, an enriched population of adult mouse primary muscle precursor cells was isolated and cultured under conditions favoring replication (33), and was treated with recombinant sCripto; cell proliferation was measured by BrdU incorporation. Physiological concentrations of recombinant sCripto increased myoblast proliferation in a dose-dependent manner (Fig. 6*A*), and addition of anti-Cripto antibodies nearly completely abolished the mitogenic effects of exogenous Cripto (Fig. 6*B*).

To investigate Cripto activity on satellite cells in a more physiological context and without bias of selection, we used isolated myofibers in culture, which provide an accessible means to study satellite cells in their native position beneath the basal lamina that surrounds each muscle fiber (26). We first performed immunofluorescence analysis for the proliferation marker Ki67 on freshly isolated myofibers treated with recombinant sCripto or left untreated as a control. In line with results on primary myoblasts, the number of proliferating Ki67$^+$ cells increased in myofibers treated with sCripto by 72 h compared with control (211 ± 6% after sCripto vs. 69 ± 3.7% after control; Fig. 6*C*), thus providing further evidence for mitogenic activity of Cripto.

Finally, given that Cripto is a GPI-anchored membrane protein in its physiological configuration (34), we also evaluated the effect of mCripto. To assess the paracrine/juxtacrine ability of mCripto further, we used single myofibers isolated from *Myf5*$^{nlacZ/+}$ mice plated on feeder layers of mammalian cells, either control or stably expressing mCripto (34), followed by counting the number of β-gal$^+$ proliferating primary myogenic cells. In keeping with our findings, β-gal$^+$ cells had almost doubled in the presence of mCripto compared with control (44 ± 0.58 vs. 22 ± 5.78, respectively; $n = 3$ independent experiments; $*P = 0.0192$; Fig. 6*D*).

Cripto Modulates Myogenic Cell Determination on Isolated Myofibers. To gain further insight into the role of Cripto on satellite cells, we performed a time course immunofluorescence analysis for Pax7 and MyoD on isolated myofibers treated with recombinant sCripto or left untreated as a control. By 48 h, supplementation of sCripto resulted in a reduced number of quiescent Pax7$^+$/MyoD$^-$ cells compared with control (Fig. 6*E*, green bars), thus suggesting that Cripto might promote/accelerate the entry of satellite cells into S phase. Moreover, by 72 h and up to 96 h in culture, the number of Pax7$^-$/MyoD$^+$ cells committed to differentiation progressively increased in sCripto-treated myofibers at the expense of Pax7$^+$/MyoD$^-$ cells (33 ± 3% for sCripto vs. 18 ± 3% of Pax7$^-$/MyoD$^+$ cells for control at 72 h, $*P < 0.05$; 48 ± 2% for sCripto vs. 23 ± 4% for control at 96 h, $**P < 0.005$; Fig. 6*E*, red bars).

We thus decided to assess whether the duration of Cripto signaling was critical for its biological activity. Isolated myofibers were then cultured in the presence of sCripto for 48 h (0–48 h), washed to remove Cripto, and cultured for the remaining 48 h (i.e., up to 96 h in total). Interestingly, the number of Pax7$^-$/

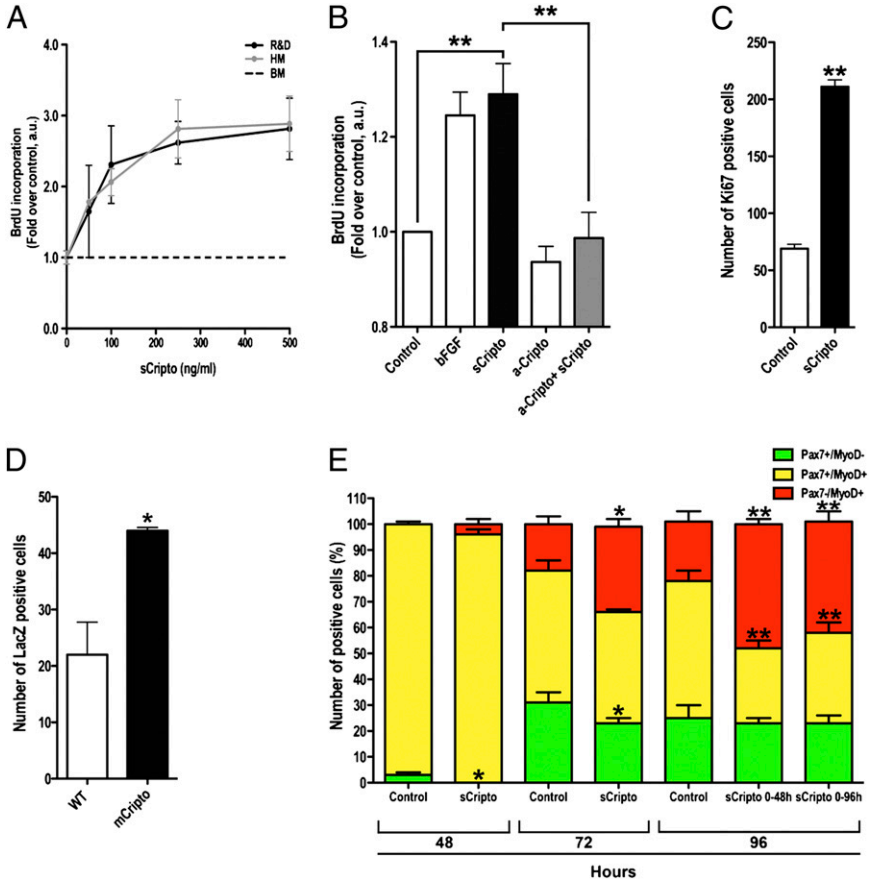

Fig. 6. Cripto promotes myoblast proliferation and modulates myogenic cell determination. (*A* and *B*) sCripto induces primary myoblast proliferation in a dose-dependent manner. Cells were cultured for 48 h in growth medium (GM curve) or in DMEM-FBS-0.5% medium containing soluble recombinant mouse Cripto (sCripto) protein using commercially available (R&D Systems) and homemade (HM) product (6–8). Activity was expressed as fold change over control/basal medium (BM; 0.5% FBS-containing medium). a.u., arbitrary unit. (*B*). Addition of anti-Cripto antibodies (R&D Systems) abolished the proproliferative effect of sCripto. Activity was expressed as fold change over control (0.5% FBS-containing medium). Basic FGF was used as a positive control; $n = 7$ independent experiments; $^{**}P = 0.05$. (*C*) Isolated myofibers treated with sCripto (200 ng/mL) for 72 h show an increased number of Ki67$^+$ proliferating cells compared with control ($n = 3$ experiments; $^{**}P < 0.001$). (*D*) Myofibers derived from *Myf5*^{nlacZ} mice plated on a feeder layer of cells stably overexpressing GPI-anchored Cripto (mCripto) show an increased number of nlacZ$^+$ myoblasts after 72 h in culture, compared with control ($n = 3$ independent experiments; $^*P = 0.0192$ vs. control). (*E*) Effect of sCripto on Pax7$^{+/-}$/MyoD$^{+/-}$ cell distribution on isolated myofibers. Double staining of fibers cultured for 48, 72, and 96 h either alone or in the presence of sCripto is shown. In the presence of sCripto, Pax7$^+$/MyoD$^-$ cells (green bar) were absent by 48 h. Pax7$^-$/MyoD$^+$ cells (red bar) progressively increased. The percentage of Pax7$^-$/MyoD$^+$ cells did not change significantly in myofibers treated with sCripto for 0–48 h, compared with control for 0–96 h ($n = 3$ independent experiments; $^*P < 0.05$; $^{**}P < 0.005$). Values are mean ± SEM. See also Fig. S5.

MyoD$^+$ cells increased to the same extent as observed for cells treated with Cripto throughout the culture (43 ± 4% for sCripto vs. 23 ± 4% for control after 96 h; $^{**}P < 0.005$; Fig. 6*E*, red bars), suggesting that treatment for 48 h is sufficient to induce an effective Cripto response.

Finally, as shown for sCripto (Fig. 6*E*), immunofluorescence analysis of isolated myofibers infected with mCripto-overexpressing lentivirus revealed an increased number of Pax7$^-$/MyoD$^+$ cells compared with lentivirus (Lenti)-Control–infected fibers at 72 h (41.8 ± 2.1% after mCripto vs. 25.9 ± 2.3% after control; $n = 3$ experiments; $^*P < 0.01$ and $^{**}P < 0.001$; Fig. S5*A*).

Taken together, our data suggest that Cripto plays a dual role, by increasing the proliferation of myogenic cells and by promoting satellite cell progression into the myogenic lineage.

Cripto Antagonizes the Effect of Myostatin/GDF8 on Satellite Cells in Isolated Myofibers. Previous findings indicated that Cripto contributes to the modulation of cell proliferation and growth by antagonizing members of the TGF-β superfamily, such as TGF-β itself or activin (15, 35). Myostatin/GDF8 is a TGF-β family member and a strong inhibitor of muscle growth, and it is expressed by quiescent satellite cells (36). To explore the molecular mechanism of Cripto signaling on satellite cells, we investigated whether Cripto may act as an antagonist of myostatin/GDF8 (GDF8). We therefore first measured the ability of GDF8 to activate Smad2 phosphorylation in the absence or presence of Cripto. To this end, 293T cells were transfected with sCripto expressing plasmid or empty control vector and were treated with increasing doses of recombinant GDF8 (Fig. 7*A*). In line with our hypothesis, GDF8-induced Smad2 phosphorylation was inhibited by sCripto, even at the highest concentrations of GDF8 tested (Fig. 7*A*). Moreover, sCripto was able to reduce GDF8-induced Smad2 phosphorylation in C2C12 myogenic cells (Fig. S5*B*). Remarkably, membrane-anchored mCripto retained its ability to antagonize GDF8 signaling (Fig. S5*C*). Furthermore, in agreement with the idea that Cripto/GDF8 may regulate satellite cell myogenic commitment, blocking GDF8 activity by adding anti-GDF8 antibodies to the fibers increased the tendency to differentiation of satellite cells, as indicated by an increased number of Pax7$^-$/MyoD$^+$ cells, at different time points (178 ± 6.0 cells for anti-GDF8 vs. 48 ± 2.4 cells for control at 72 h; $^{**}P = 0.005$; Fig. 7*B*). Moreover, addition of sCripto to anti-GDF8–treated myofibers did not further increase

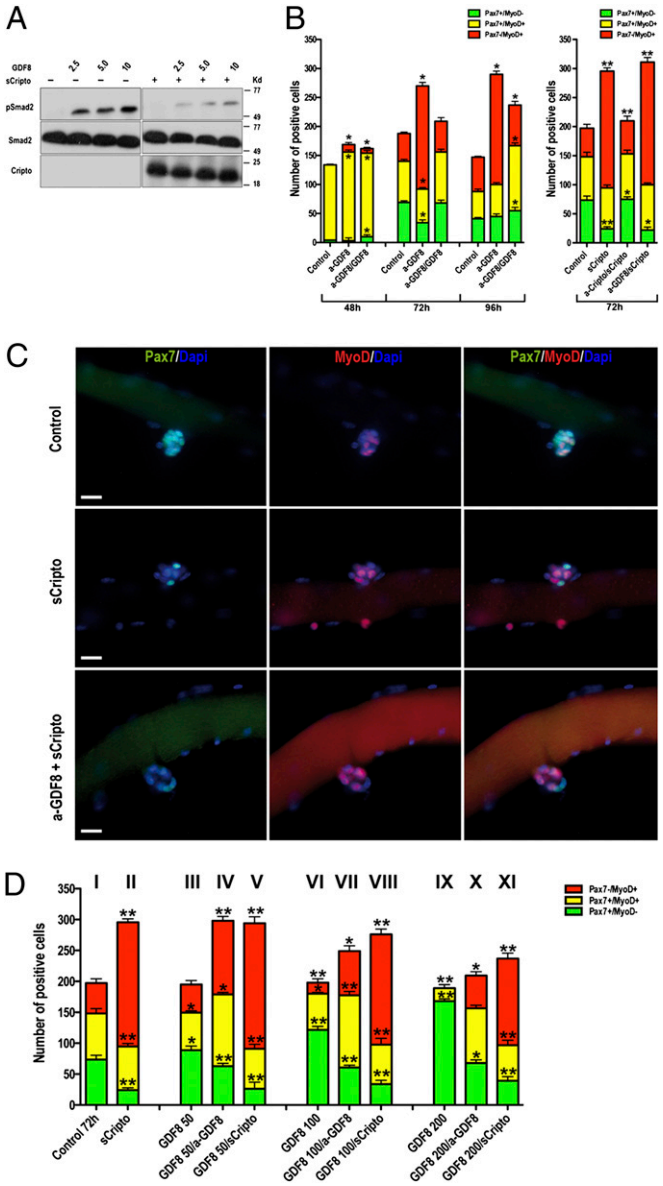

Fig. 7. Cripto antagonizes myostatin/GDF8 signaling and counteracts its antiproliferative effect on satellite cells. (*A*) sCripto overexpression reduces myostatin/GDF8-induced Smad2 phosphorylation. Total lysates of 293T cells, transfected with empty- or sCripto-vector and treated with increasing doses of myostatin/GDF8 (R&D Systems), were subjected to Western blot analysis using anti–phospho (P)-Smad2, -Smad2, or -Cripto antibodies. (*B–D*) Cripto/GDF8 signaling interaction expanded the pool of satellite cells committed to myogenic lineage. (*B*) Double staining of fibers cultured for 48, 72, and 96 h, either alone or in the presence of anti-GDF8 antibodies and ± GDF8 protein (*Left*), or cultured for 72 h with sCripto and anti-GDF8 or anti-Cripto antibodies, either alone or in combination (*Right*). (*Left*) Number of $Pax7^-/MyoD^+$ committed cells (red bar) increases in fibers treated with anti-GDF8 antibodies at all time points, and the effect is antagonized by GDF8. (*Right*) Similarly, $Pax7^-/MyoD^+$ cells (red bar) increase in fibers treated with sCripto, and do not further increase in the presence of anti-GDF8, at 72 h ($n = 3$ independent experiments; $^*P < 0.05$ compared with control; $^{**}P < 0.005$ compared with control). Values are mean ± SEM. (*C*) Representative photos from single fibers treated with sCripto ± 1 h of pretreatment with anti-GDF8 antibodies and stained for Pax7 (green) and MyoD (red). (Scale bars = 50 μm.) (*D*) Functional titration of GDF8 activity on isolated fibers at 72 h. GDF8 increases the number of $Pax7^+/MyoD^-$ quiescent/self-renewed cells in a dose-dependent manner (50–200 ng/mL; green; bars III, VI, and IX) compared with control. Fiber pretreatment with either anti-GDF8 blocking antibodies (bars IV, VII, and X) or sCripto (bars V, VIII, and XI) blocks the antiproliferative effect of GDF8 ($n = 3$ independent experiments; $^*P < 0.05$; $^{**}P < 0.005$). Values are mean ± SEM. See also Fig. S5.

$Pax7^-/MyoD^+$ cell number (211 ± 8.0 cells; $^{**}P = 0.005$; Fig. 7*B*, red bars).

We then investigated whether there was a functional interaction between Cripto and GDF8 signaling pathways on isolated myofibers. As expected, sCripto treatment resulted in an increased number of $Pax7^-/MyoD^+$ cells by 72 h in culture (201 ± 5.5 cells with sCripto vs. 49 ± 6.7 cells with control; $n = 7$ independent experiments; $^{**}P = 0.005$; Fig. 7 *B* and *C*). We next asked whether Cripto might directly antagonize the effect of GDF8 (50–200 ng/mL; R&D Systems) on satellite cell determination. As expected, GDF8 treatment increased the number of $Pax^+/MyoD^-$ quiescent and/or self-renewed satellite cells on isolated myofibers, at the expense of $MyoD^+$ cells, in a dose-dependent manner (88.67 ± 6.7 cells, 121.4 ± 5.9 cells, and 168 ± 3.8 cells at 50, 100, and 200 ng/mL, respectively; Fig. 7*D*, bars III, VI, and IX). On the other hand, addition of anti-GDF8 blocking antibodies blocked the antiproliferative effect of GDF8 and expansion of the pool of satellite cells committed to myogenic lineage (Fig. 7*D*, bars IV, VII, and X). Most interestingly, addition of sCripto (200 ng/mL) almost completely reversed the outcome of GDF8 treatment on cell proliferation as well as on $Pax7^{+/-}/MyoD^{+/-}$ satellite cell distribution, even at the highest concentration of GDF8 used (i.e., 200 ng/mL; Fig. 7*D*, bars V, VIII, and XI).

Consistent with the idea that Cripto could act as an antagonist of myostatin/GDF8, we showed that Cripto and myostatin are expressed in regenerating muscles (Fig. S5 *D* and *E*). Together, these data revealed a functional interaction between Cripto and myostatin/GDF8 signaling pathways to modulate myogenic cell determination.

Discussion

The capacity of the skeletal muscle regenerative response is primarily due to a resident population of myogenic stem cells, the satellite cells. It is well known that extrinsic and intrinsic signaling pathways modulate the status of the satellite cell pool (37); however, the molecular mechanisms are not yet fully defined.

Here, we demonstrate that Cripto, a critical signal in embryonic development, is reexpressed in adult skeletal muscles that undergo regeneration and that its activity can modulate skeletal muscle regeneration. We show that Cripto is undetectable in quiescent $Pax7^+/MyoD^-$ satellite cells but that it accumulates in activated satellite cells, being coexpressed with myogenic lineage markers, such as Pax7, Myf5, and MyoD, thus suggesting that Cripto expression occurs concomitantly and/or following activation of satellite cells. Interestingly, Cripto is also expressed in inflammatory cells during regeneration. Notably, in addition to myogenic cells, inflammatory cells, which are recruited to the damaged area, provide an important contribution to muscle regeneration. Indeed, recent studies have shown that factors expressed during the inflammatory process can influence skeletal muscle regeneration by stimulating satellite cell survival and/or proliferation (38, 39). For example, recent data provided evidence that infiltrating inflammatory cell-derived granulocyte colony-stimulating factor enhances myoblast proliferation and facilitates skeletal muscle regeneration, thereby underscoring the importance of inflammation-mediated induction of muscle regeneration (39). Conditional Cripto inactivation in adult satellite cells allowed us to unmask the cellular contribution of Cripto in vivo and provide previously undescribed evidence for a functional role of this protein during muscle regeneration. Notably, although our data do not rule out the possibility that Cripto expressed by infiltrating macrophages would also contribute to this effect, our findings simply indicate that this was not sufficient to compensate for the lack of Cripto in satellite cells.

In line with these findings, we demonstrate that Cripto modulates the different fates of satellite cells and that it is mitogenic for satellite cell-derived myoblasts. To address this issue, we used

isolated myofibers in culture, which allows investigation of the effect of exogenous factors on satellite cells in their native positions (26), and found that exposure to either sCripto or GPI-anchored Cripto increased the number of $Pax7^-/MyoD^+$ committed myogenic cells at the expense of $Pax7^+/MyoD^-$ cells, suggesting that Cripto promotes/accelerates the entry of satellite cells into S phase and their commitment to differentiation. Moreover, we show that Cripto promotes proliferation both in isolated myofibers and in primary myoblasts in culture. This notion is consistent with previous findings that support a model in which Cripto possesses intrinsic activities as a transacting factor both in cell culture and in vivo (6–8, 31). In line with this idea, sCripto was able to rescue fully the effect on muscle regeneration of the genetic ablation of *cripto* in adult satellite cells. This represents in vivo evidence in the mouse that sCripto recapitulates the function of GPI-anchored Cripto.

Several molecules have been described that regulate stem cell proliferation and/or differentiation, and eventually muscle regeneration, including those belonging to the TGF-β superfamily (11). Interestingly, in addition to its obligate role as a Nodal/GDF1/GDF3 coreceptor, Cripto can antagonize signaling by activins and TGF-β (13–15). GDF8/myostatin is a member of the TGF-β superfamily that has been implicated in the negative regulation of muscle growth and regeneration (36). Consistent with the idea that Cripto could act as an antagonist of myostatin/GDF8, we show that Cripto and myostatin are expressed in regenerating muscles and, most remarkably, that (*i*) both secreted and membrane-anchored Cripto is able to attenuate the myostatin/Smad2 signaling pathway; (*ii*) Cripto antagonizes the antiproliferative effect of myostatin on isolated myofibers, promoting myogenic commitment; and, similarly, (*iii*) blocking myostatin activity increases the tendency toward differentiation of satellite cells.

Myostatin is expressed by quiescent satellite cells and has a functional role in repressing satellite cell proliferation and enhancing self-renewal (40). A number of factors have been discovered that antagonize myostatin activity, such as follistatin (24), recently suggested to induce muscle hypertrophy through satellite cell proliferation and inhibition of both myostatin and activin (41). However, the direct relevance of myostatin for satellite cells is still debated, and controversial models have been proposed regarding which cell types mediate the effects of myostatin on muscle physiology (41, 43).

Several lines of evidence suggested that the normal function of myostatin in adult muscle is to maintain satellite cells in a quiescent state, acting as a negative regulator of cell activation and proliferation (36, 44, 45). Moreover, studies in chick and mouse embryos pointed to a context-dependent effect of myostatin, controlling the balance between proliferation and differentiation on muscle progenitors (46). In contrast, recent data indicate that postnatal muscle hypertrophy generated by the lack of myostatin is largely due to hypertrophy of individual fibers and not to satellite cell activity (47). Indeed, it has been reported that the addition of recombinant myostatin (100 ng/mL) does not influence satellite cell proliferation in vitro. Notably, in that study, myostatin was added to isolated fibers after 48 h in culture and maintained over the subsequent 24 h (47). Our protocol differs from this in that sCripto and/or myostatin (50–200 ng/mL) was added to myofibers immediately after culture, which might explain the apparent discrepancy. We found that in this experimental setting, myostatin is able to inhibit and/or delay the progression of $Pax7^+/MyoD^-$ quiescent satellite cells toward $Pax7^+/MyoD^+$ myogenic/proliferating cells. Interestingly, this effect is reverted by sCripto and also persists on removal of Cripto after 48 h. Although we cannot rule out the possibility that residual Cripto might remain bound to the fibers/cells, thus explaining the long-lasting effect of the treatment, previous findings in ESCs showed that the transient presence of sCripto in the early time window of differentiation (0–48 h) was sufficient to rescue the cardiac phenotype of $cripto^{-/-}$ ESCs fully at later time points (31).

In conclusion, we identified Cripto as a factor required for efficient repair of skeletal muscles and propose that Cripto regulates satellite cell progression toward the myogenic lineage, at least in part, by counteracting myostatin activity. Although we cannot rule out the possibility that other signaling pathways might also be involved, our intriguing findings are in line with very recent data, which report that overexpression of Cripto antagonized myostatin-induced A3 luciferase activity in 293T cells (48). In contrast to these findings, it has recently been proposed that Cripto may also exert a stimulatory role on myostatin signaling, suggesting that Cripto-mediated myostatin signaling is dose-dependent (49). Although further experiments will be necessary to elucidate the molecular basis of this newly identified Cripto/myostatin interaction, our study indicates that this could represent a novel mechanism for the control of satellite cell decisions necessary for robust skeletal muscle maintenance and repair.

Finally, our findings that Cripto is expressed in both myogenic and inflammatory cells places Cripto within a complex regulatory network that links inflammation and skeletal muscle regeneration, a relationship that remains incompletely understood, and thus opens the way to assess the potential of Cripto as target for the treatment of skeletal muscle injury or disease.

Experimental Procedures

Section Immunostaining. Muscles were freshly frozen and cut in cryostat sections. Slides were fixed in 4% (wt/vol) paraformaldehyde (PFA), permeabilized with 0.5% Triton X-100 (Sigma–Aldrich), and boiled 15 min in 10 mM sodium citrate. Primary antibodies used are as follows: anti-Cripto (6–7 μg/mL; 1:50, Santa Cruz Biotechnology; 1:150, Abcam), antilaminin (1:50; Abcam), anti-MyoD (1:20; Dako), F4/80 (1:50; Serotec), and desmin (1:50, ICN). Appropriate fluorophore-conjugated secondary antibodies, Alexa Fluor 488 and Alexa Fluor 594 (1:300; Molecular Probes) or HRP conjugated (DAKO) and fluorescein-labeled thyramide (PerkinElmer) were used for visualization. Vectashield medium containing DAPI (Vector Laboratories) was used for mounting. Sections incubated without primary antibodies served as controls. Labeling was visualized by epifluorescent illumination using an Axiovision microscope (Carl Zeiss), and images were acquired on an Axiocam camera (Carl Zeiss) or a DFC480 or DFC350FX camera (Leica).

Isolation and Growth of Mouse Primary Myoblasts. Purification of primary myoblast culture was performed as previously described (33, 50). Details are provided in *SI Experimental Procedures*.

Cell Proliferation Assays. Myoblasts were cultured at 5×10^4 cells per well on 96-well microtiter plates in growth medium for a few hours and then serum starved overnight in DMEM with 0.5% FBS. After washing, cells were cultured in DMEM-FBS-0.5% medium containing soluble recombinant mouse Cripto (sCripto) at 5, 50, 100, 250, or 500 ng/mL (R&D Systems) and a homemade product (6), human basic FGF (10 ng/mL; R&D Systems), or neutralizing antibodies at 4 μg/mL (anti-Cripto, MAB1538; R&D Systems). A BrdU cell proliferation assay kit (Roche) was used following the manufacturer's instructions. BrdU incorporation was measured by the absorbance of the samples in an ELISA reader at 370 nm (reference wavelength of ~492 nm).

Single-Fiber Culture Assays. Single floating myofibers were prepared from the extensor digitorum longus (EDL) muscles from 6-wk-old C57/Bl6 or *Myf5*$^{nlacZ/+}$ mice (27, 51), as described (26, 52). Individual intact myofibers were placed in horse serum (HS)-coated, round-bottomed Eppendorf tubes and incubated with or without mouse sCripto (200 ng/mL; R&D Systems) or myostatin/GDF8 (50, 100, or 200 ng/mL; R&D Systems) in low-activation medium [10% (vol/vol) HS and 0.5% chicken embryo extract (CEE) in DMEM]. Myofibers were treated with sCripto or preincubated for 1 h with either blocking anti-Cripto (MAB1538, 4 μg/mL; R&D Systems) or anti-myostatin/GDF8 (GT15213, 10 μg/mL; Neuromics) antibodies before Cripto addition.

In the anti-GDF8 time course experiment, myofibers were incubated for 48, 72, or 96 h with anti-GDF8 (GT15213, 10 μg/mL) either alone or preincubated for 1 h with GFD8 (200 ng/mL). After 48 or 72 h of treatment, floating fibers were fixed in 4% (wt/vol) PFA, rinsed in PBS, and immediately used for immunostaining. Primary antibodies used are as follows: MyoD (1:50; Dako

or Santa Cruz Biotechnology), Pax7 [1:10; Developmental Studies Hybridoma Bank (DSHB)] (26), β-gal (1:350; Biogenesis), and Ki67 (1:250; Abcam) (53).

Alternatively, *Myf5*$^{nlacZ/+}$ myofibers were plated on a feeder layer of mammalian cells expressing membrane-bound Cripto or a mock vector in a 24-multiwell plate in proliferating medium (20% (vol/vol) FBS, 10% (vol/vol) HS, and 1% CEE in DMEM). LacZ staining was performed after 72 h to identify activated satellite cells on the fibers and those that have left the fibers.

Mice and Genotyping. The *Cripto*$^{loxP/-}$ mice were generated by crossing *Cripto*$^{loxP/loxP}$ (8) and *Cripto*$^{+/-}$ (54) animals and were genotyped by PCR analysis with specific oligos that generate a 197-bp band [allele (–)] and a 580-bp band [allele (loxP)]. The *Tg:Pax7-CreERT2::Cripto*$^{loxP/-}$ mice were generated by crossing *Pax7-CreERT2* (30) and *Cripto*$^{loxP/-}$ animals and genotyped by PCR with primers mapping on *Cre* sequence, generating a 600-bp band. The *Cripto* floxed allele (Cripto Del) is detected as a 600-bp band. Genotyping strategies of Cripto$^{loxP/loxP}$ (8) and Cripto$^{+/-}$ (54) have been published. Primer sequences are shown in Table S1.

Muscle Injections, Preparation, and Analysis. Ten microliters of CTX (10E-3M or 10E-5M in PBS) were injected in the tibialis anterior (TA) from 8-wk-old Balbc mice, in the CTX mouse models of more severe or less severe muscle damage, respectively. Following CTX injection, mice were injected i.m. with Ad-sCripto, generated using the AdEasy XL System (Stratagene), or with Ad-Control (4×10^9 pfu, in a total volume of 25 μL), and muscles were harvested at the indicated time points after damage.

Adult (1 mo of age) Tg:Pax7-CreERT2::CriptoloxP/$^{-}$ and CriptoloxP/$^{-}$ mice were injected i.p. with tamoxifen (T5648, 60 mg/g per day, Sigma–Aldrich) or sesame oil (S3547; Sigma–Aldrich), as a control vehicle, once a day for 5 d. On day 4, 15 microliters of CTX (10E-5M in PBS) was injected into the TA muscle. In the rescue experiment, following CTX injection, mice were injected i.m. with either Ad-sCripto or Ad-Control. For morphological and morphometric analysis, muscles were either embedded unfixed in Sakura Tissue-Tek oct (Gentaur) and frozen in isopentane-cooled liquid nitrogen for cryosection or fixed in PFA and embedded in paraffin. Tissue necrosis was identified by morphological alterations of myofibers (i.e., hypercontraction) or loss of sarcolemmal integrity and by the presence of cellular debris in the surrounding interstitial space (55). Regenerated myofibers were identified by the presence of central nuclei, and the diameter or CSA of fibers was morphometrically analyzed using KS300 image analysis software (Carl Zeiss) or ImageQuant software (QWin; Leica).

DNA Plasmids, Cell Culture, and Western Blot. sCripto and mCripto were previously described (6, 34). Briefly, mCripto corresponds to the full-length cripto cDNA, whereas sCripto corresponds to cripto cDNA with a STOP codon at nucleotide +156.

293T or C2C12 cells were plated on six-well plates at a density of 2×10^5. Twenty-four hours after plating, cells were transfected with 4 μg of DNA (pCDNA3, pCDNA3-sCripto, and pCDNA3-mCripto) using lipofectamine (Invitrogen). Twenty-four hours after transfection, cells were serum-starved for 8 h before treatment. Cells were left untreated or were treated for 30 min with the indicated doses of myostatin/GDF8 protein (R&D Systems). Total protein extracts were prepared and analyzed by Western blot as previously described (56). Anti–phospho-Smad2, Smad2 (Cell Signaling Technology), and Cripto antibodies (R&D Systems) were used as previously described (31).

RNA Preparation and RT-PCR. Total RNAs from the TA muscle were isolated using an RNeasy mini kit (Qiagen) according to the manufacturer's instruction. One microgram of total RNA was utilized for cDNA synthesis using SuperScript II reverse transcriptase (Life Technologies) and random hexamers. A qRT-PCR assay was performed using SYBR Green PCR master mix (EuroClone). Primers are listed in Table S2.

Statistical Analysis. All values are expressed as mean ± SEM. To determine significance between two groups, comparisons were made using unpaired Student *t* tests. Analyses of multiple groups were performed utilizing paired Student *t* tests using Prism version 5.00 for Mac (GraphPad Software). $P < 0.05$ was considered statistically significant.

ACKNOWLEDGMENTS. We thank the Animal House, the Integrated Microscopy facilities and the FACS facilities of the Institute of Genetics and Biophysics "Adriano Buzzati-Traverso," Consiglio Nazionale delle Ricerche, for technical assistance; Sabine Wyns for help in generating Cripto-adenovirus; and Ann Carton for technical support. This work was supported by the European Community's Seventh Framework Programme for the ENDOSTEM project (Activation of Vasculature-Associated Stem Cells and Muscle Stem Cells for the Repair and Maintenance of Muscle Tissue, Grant 241440) (to G.M. and S.B.); Telethon (Grant GGP08120); Associazione Italiana per la Ricerca sul Cancro, Ministero I struzione Università Ricerca (Medical Research in Italy, Grant RBNE08HM7T_003) (to G.M.); and Association Française contre les Myopathies (G.M., P.C., P.L., and S.T.). PL was supported by a European Molecular Biology Organization Long-Term Fellowship.

1. Beachy PA, Karhadkar SS, Berman DM (2004) Tissue repair and stem cell renewal in carcinogenesis. *Nature* 432(7015):324–331.
2. Shen MM, Schier AF (2000) The EGF-CFC gene family in vertebrate development. *Trends Genet* 16(7):303–309.
3. Assou S, et al. (2007) A meta-analysis of human embryonic stem cells transcriptome integrated into a web-based expression atlas. *Stem Cells* 25(4):961–973.
4. Minchiotti G (2005) Nodal-dependant Cripto signaling in ES cells: From stem cells to tumor biology. *Oncogene* 24(37):5668–5675.
5. Miharada K, et al. (2011) Cripto regulates hematopoietic stem cells as a hypoxic-niche-related factor through cell surface receptor GRP78. *Cell Stem Cell* 9(4):330–344.
6. Minchiotti G, et al. (2001) Structure-function analysis of the EGF-CFC family member Cripto identifies residues essential for nodal signalling. *Development* 128(22):4501–4510.
7. Bianco C, et al. (2002) Cripto-1 activates nodal- and ALK4-dependent and -independent signaling pathways in mammary epithelial Cells. *Mol Cell Biol* 22(8):2586–2597.
8. Chu J, et al. (2005) Non-cell-autonomous role for Cripto in axial midline formation during vertebrate embryogenesis. *Development* 132(24):5539–5551.
9. Reissmann E, et al. (2001) The orphan receptor ALK7 and the Activin receptor ALK4 mediate signaling by Nodal proteins during vertebrate development. *Genes Dev* 15 (15):2010–2022.
10. Cheng SK, Olale F, Bennett JT, Brivanlou AH, Schier AF (2003) EGF-CFC proteins are essential coreceptors for the TGF-beta signals Vg1 and GDF1. *Genes Dev* 17(1):31–36.
11. Shi X, Garry DJ (2006) Muscle stem cells in development, regeneration, and disease. *Genes Dev* 20(13):1692–1708.
12. Massagué J, Chen YG (2000) Controlling TGF-beta signaling. *Genes Dev* 14(6): 627–644.
13. Adkins HB, et al. (2003) Antibody blockade of the Cripto CFC domain suppresses tumor cell growth in vivo. *J Clin Invest* 112(4):575–587.
14. Gray PC, Harrison CA, Vale W (2003) Cripto forms a complex with activin and type II activin receptors and can block activin signaling. *Proc Natl Acad Sci USA* 100(9):5193–5198.
15. Gray PC, Shani G, Aung K, Kelber J, Vale W (2006) Cripto binds transforming growth factor beta (TGF-beta) and inhibits TGF-beta signaling. *Mol Cell Biol* 26(24):9268–9278.
16. Adamson ED, Minchiotti G, Salomon DS (2002) Cripto: A tumor growth factor and more. *J Cell Physiol* 190(3):267–278.
17. Strizzi L, Bianco C, Normanno N, Salomon D (2005) Cripto-1: A multifunctional modulator during embryogenesis and oncogenesis. *Oncogene* 24(37):5731–5741.
18. Chargé SB, Rudnicki MA (2004) Cellular and molecular regulation of muscle regeneration. *Physiol Rev* 84(1):209–238.
19. Seale P, et al. (2000) Pax7 is required for the specification of myogenic satellite cells. *Cell* 102(6):777–786.
20. Tedesco FS, et al. (2011) Stem cell-mediated transfer of a human artificial chromosome ameliorates muscular dystrophy. *Sci Transl Med* 3(96):96ra78.
21. Tajbakhsh S (2005) Skeletal muscle stem and progenitor cells: Reconciling genetics and lineage. *Exp Cell Res* 306(2):364–372.
22. Tatsumi R, Anderson JE, Nevoret CJ, Halevy O, Allen RE (1998) HGF/SF is present in normal adult skeletal muscle and is capable of activating satellite cells. *Dev Biol* 194 (1):114–128.
23. Musarò A, Rosenthal N (1999) Maturation of the myogenic program is induced by postmitotic expression of insulin-like growth factor I. *Mol Cell Biol* 19(4): 3115–3124.
24. Lee SJ, McPherron AC (2001) Regulation of myostatin activity and muscle growth. *Proc Natl Acad Sci USA* 98(16):9306–9311.
25. Otto A, et al. (2008) Canonical Wnt signalling induces satellite-cell proliferation during adult skeletal muscle regeneration. *J Cell Sci* 121(Pt 17):2939–2950.
26. Zammit PS, et al. (2004) Muscle satellite cells adopt divergent fates: A mechanism for self-renewal? *J Cell Biol* 166(3):347–357.
27. Beauchamp JR, et al. (2000) Expression of CD34 and Myf5 defines the majority of quiescent adult skeletal muscle satellite cells. *J Cell Biol* 151(6):1221–1234.
28. Tajbakhsh S, Rocancourt D, Buckingham M (1996) Muscle progenitor cells failing to respond to positional cues adopt non-myogenic fates in myf-5 null mice. *Nature* 384 (6606):266–270.
29. Ding J, et al. (1998) Cripto is required for correct orientation of the anterior-posterior axis in the mouse embryo. *Nature* 395(6703):702–707.
30. Mourikis P, et al. (2011) A critical requirement for notch signaling in maintenance of the quiescent skeletal muscle stem cell state. *Stem Cells* 30(2):243–252.
31. Parisi S, et al. (2003) Nodal-dependent Cripto signaling promotes cardiomyogenesis and redirects the neural fate of embryonic stem cells. *J Cell Biol* 163(2):303–314.
32. Arsic N, et al. (2003) Induction of functional neovascularization by combined VEGF and angiopoietin-1 gene transfer using AAV vectors. *Mol Ther* 7(4):450–459.
33. Qu Z, et al. (1998) Development of approaches to improve cell survival in myoblast transfer therapy. *J Cell Biol* 142(5):1257–1267.

34. Minchiotti G, et al. (2000) Membrane-anchorage of Cripto protein by glycosylphosphatidylinositol and its distribution during early mouse development. *Mech Dev* 90(2):133–142.
35. Shen MM (2003) Decrypting the role of Cripto in tumorigenesis. *J Clin Invest* 112(4): 500–502.
36. Thomas M, et al. (2000) Myostatin, a negative regulator of muscle growth, functions by inhibiting myoblast proliferation. *J Biol Chem* 275(51):40235–40243.
37. Jang YC, Sinha M, Cerletti M, Dall'Osso C, Wagers AJ (2011) Skeletal muscle stem cells: Effects of aging and metabolism on muscle regenerative function. *Cold Spring Harb Symp Quant Biol* 76:101–111.
38. Chazaud B, et al. (2003) Satellite cells attract monocytes and use macrophages as a support to escape apoptosis and enhance muscle growth. *J Cell Biol* 163(5): 1133–1143.
39. Hara M, et al. (2011) G-CSF influences mouse skeletal muscle development and regeneration by stimulating myoblast proliferation. *J Exp Med* 208(4):715–727.
40. McCroskery S, et al. (2003) Myostatin negatively regulates satellite cell activation and self-renewal. *J Cell Biol* 162(6):1135–1147.
41. Gilson H, et al. (2009) Follistatin induces muscle hypertrophy through satellite cell proliferation and inhibition of both myostatin and activin. *Am J Physiol Endocrinol Metab* 297(1):E157–E164.
42. Cassano M, et al. (2009) Cellular mechanisms and local progenitor activation to regulate skeletal muscle mass. *J Muscle Res Cell Motil* 30(7-8):243–253.
43. Bentzinger CF, von Maltzahn J, Rudnicki MA (2010) Extrinsic regulation of satellite cell specification. *Stem Cell Res Ther* 1(3):27.
44. Joulia D, et al. (2003) Mechanisms involved in the inhibition of myoblast proliferation and differentiation by myostatin. *Exp Cell Res* 286(2):263–275.
45. Amthor H, Otto A, Macharia R, McKinnell I, Patel K (2006) Myostatin imposes reversible quiescence on embryonic muscle precursors. *Dev Dyn* 235(3):672–680.
46. Manceau M, et al. (2008) Myostatin promotes the terminal differentiation of embryonic muscle progenitors. *Genes Dev* 22(5):668–681.
47. Amthor H, et al. (2009) Muscle hypertrophy driven by myostatin blockade does not require stem/precursor-cell activity. *Proc Natl Acad Sci USA* 106(18):7479–7484.
48. Ciarmela P, et al. (2011) Activin-A and myostatin response and steroid regulation in human myometrium: Disruption of their signalling in uterine fibroid. *J Clin Endocrinol Metab* 96(3):755–765.
49. Kemaladewi DU, et al. (2012) Cell-type specific regulation of myostatin signaling. *FASEB J* 26(4):1462–1472.
50. Rando TA, Blau HM (1994) Primary mouse myoblast purification, characterization, and transplantation for cell-mediated gene therapy. *J Cell Biol* 125(6):1275–1287.
51. Montarras D, et al. (2005) Direct isolation of satellite cells for skeletal muscle regeneration. *Science* 309(5743):2064–2067.
52. Rosenblatt JD, Lunt AI, Parry DJ, Partridge TA (1995) Culturing satellite cells from living single muscle fiber explants. *In Vitro Cell Dev Biol Anim* 31(10):773–779.
53. Abou-Khalil R, et al. (2009) Autocrine and paracrine angiopoietin 1/Tie-2 signaling promotes muscle satellite cell self-renewal. *Cell Stem Cell* 5(3):298–309.
54. Xu C, et al. (1999) Abrogation of the Cripto gene in mouse leads to failure of postgastrulation morphogenesis and lack of differentiation of cardiomyocytes. *Development* 126(3):483–494.
55. Ferreira R, et al. (2009) Proteolysis activation and proteome alterations in murine skeletal muscle submitted to 1 week of hindlimb suspension. *Eur J Appl Physiol* 107(5): 553–563.
56. Kelber JA, Shani G, Booker EC, Vale WW, Gray PC (2008) Cripto is a noncompetitive activin antagonist that forms analogous signaling complexes with activin and nodal. *J Biol Chem* 283(8):4490–4500.